Interventional Causal Identification of Dissolution-Buffered Gas Influx in Managed Pressure Drilling

Hamza Qureshi[1] **and Bilal Mahmood**[2]

[1]University of Lakki Marwat, Tajazai Road, Lakki Marwat 28420, Khyber Pakhtunkhwa, Pakistan

[2] Khwaja Fareed University of Engineering and Information Technology, Abu Dhabi Road, Rahim Yar Khan 64200, Punjab, Pakistan

ABSTRACT

Managed pressure drilling operates the wellbore as an actively actuated hydraulic system in which choke and pump commands continually reshape pressure and flow signals. This operating mode reduces large excursions but makes early gas influx discrimination more difficult because the dominant surface observables are simultaneously driven by control interventions, compressible storage, frictional variability, and multiphase inventory changes. In oil-based and synthetic-based fluids, part of an invading gas mass can dissolve into the circulating liquid and induce swelling, producing pit-volume and density shifts without an immediately dominant free-gas holdup. This paper formulates influx diagnosis as an interventional causal identification problem rather than as a residual-threshold task. The technical contribution is a structural causal model for annular hydraulics with thermodynamics-augmented latent inventories, paired with an invariant-causal learning objective that exploits routine control interventions as quasi-experiments. A constrained causal discovery layer identifies a minimal adjustment set for influx effects under partial observability and sensor bias, while a counterfactual simulator computes risk-relevant outcomes under hypothetical choke trajectories. The method separates actuation-induced transients from influx-driven signatures by enforcing invariance of causal mechanisms across intervention regimes and by penalizing spurious predictive paths that fail under do-operations. A practical estimation algorithm is derived using intervention-conditioned variational inference with inequality-consistent parameterizations for phase partition and swelling. Numerical studies demonstrate improved separation of swelling-consistent pit gain from free-gas-driven compressibility, stable behavior under intermittent telemetry and closure mismatch, and calibrated counterfactual risk estimates for short-horizon decision support.

1. Introduction

Managed pressure drilling has transformed the operational landscape for wells with narrow margins by shifting the hydraulic regime from passive to actively actuated [1]. Choke backpressure and pump schedules are adjusted continuously to shape bottomhole pressure trajectories, reduce the probability of large deviations, and maintain circulation objectives. From an inference perspective, however, this success introduces a structural complication: the same boundary interventions used to stabilize the system become the primary drivers of the very signals used for diagnosis. Surface pressure, flow-out, and pit-volume trajectories become mixtures of (i) the causal response to deliberate interventions, (ii) the response to unmodeled disturbances such as cuttings loading and rheology drift, (iii) the response to latent multiphase inventory changes, and (iv) sensor bias and filtering. In this setting, a purely correlational detector can perform poorly even when it is statistically sophisticated, because correlation

Article info:
Hamza Qureshi and Bilal Mahmood. *Interventional Causal Identification of Dissolution-Buffered Gas Influx in Managed Pressure Drilling*. Helikonpress. Publishing. Licensed under Attribution - NonCommercial - No Derivatives 4.0 International (CC BY-NC-ND 4.0)

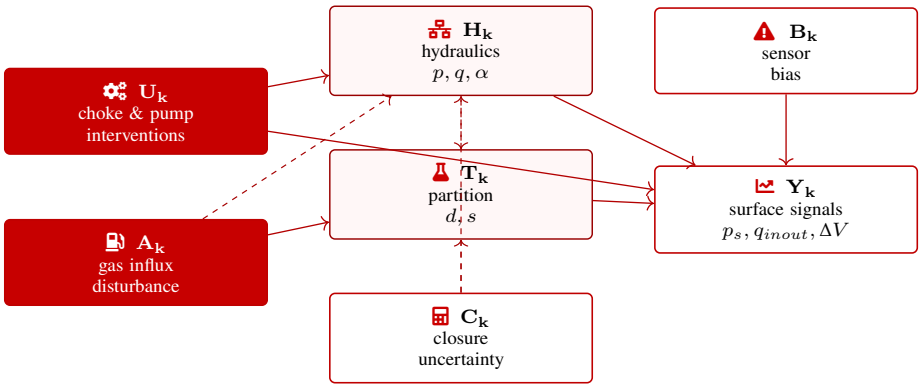


Figure 1 Interventional SCM overview. Controlled actuation U_k drives hydraulics while influx A_k perturbs latent inventories. Thermodynamic partition d, s mediates swelling-like volumetric signatures distinct from free-gas compressibility. Bias states and closure uncertainty are explicit to avoid spurious attribution under active managed-pressure control.

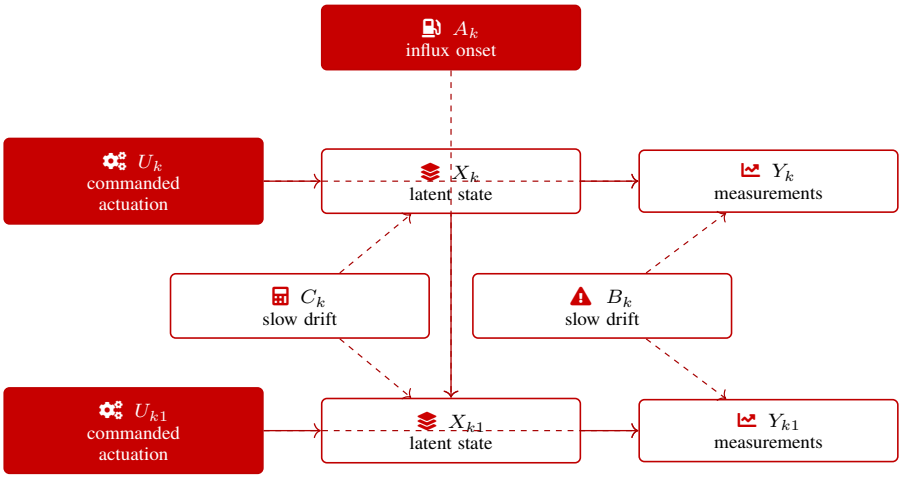


Figure 2 Dynamic SCM slice (two-step view). State propagation carries hydraulic and thermodynamic inventories forward while interventions enter as externally set boundary conditions. Slow-drift closure parameters and sensor bias states are modeled as separate latent processes influencing dynamics and measurements without being mistaken for influx.

patterns can be altered by routine interventions and can differ across operating envelopes without any influx occurring.

A second complication is thermodynamic partitioning of gas mass between free and dissolved inventories. Early-stage influx in oil-based and synthetic-based systems can be buffered by dissolution, producing liquid swelling and altered volumetric returns without immediate formation of a large free-gas holdup [2]. The consequence is that two latent regimes can generate similar early pit trends: a regime in which free gas accumulates and migrates upward, and a regime in which a comparable gas mass is largely dissolved at depth and expressed primarily through swelling and density modification. The operational response to these regimes can differ because the near-term risks differ, yet common heuristics can map both regimes to the same alarm condition. A mechanistic view of this ambiguity is supported by the thermodynamic modeling literature; for instance, Manikonda et al. (2020) [3] introduced an initial thermodynamics-based formulation that, for the first time, enabled operational estimation of gas-kick dissolution effects in oil-based drilling fluids and their volumetric implications for interpreting pit behavior. The present work does not seek to reproduce a full thermodynamic solver online, but it treats dissolution buffering as an explicit latent mechanism that must be accounted for when interpreting intervention-driven transients.

Beyond dissolution, closure uncertainty also challenges inference. Transient predictions depend on gas density, gas viscosity, and related PVT properties that enter hydrostatic and frictional gradients, and small correlation errors can accumulate into materially different pressure and flow predictions over the annulus. This is particularly damaging in managed pressure drilling because the operating point can sit near constraints, so small prediction errors can alter decisions [4]. Empirical evaluations indicate that nontrivial residual errors remain even for comparatively accurate correlations in high-pressure high-temperature ranges (Sleiti et al., 2021) [5]. Rather than treat closure mismatch as an additive noise term at the output, this paper represents closure uncertainty as structural uncertainty in specific causal mechanisms and uses invariance across interventions to reduce sensitivity to such mismatch.

The thesis of the paper is that early influx discrimination un-

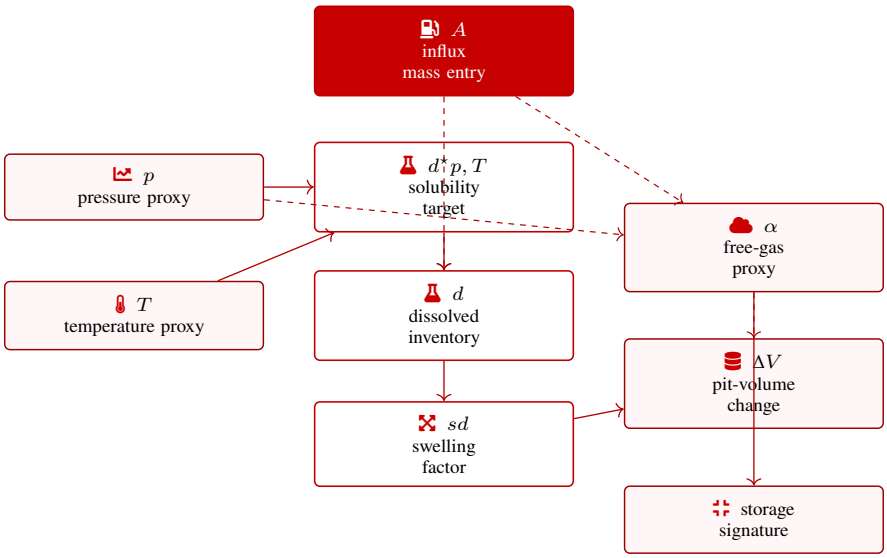


Figure 3 Latent partition mechanism for dissolution buffering. A reduced thermodynamic pathway maps p, T to a solubility target $d^\star$, relaxing into dissolved inventory d that drives swelling factor s. In parallel, free-gas proxy α drives compressible-storage signatures. Both pathways can perturb pit-volume response, but with distinct causal footprints under pressure actuation.

Symbol	Description	Causal role
U_k	Choke and pump commands	Manipulated intervention
X_k	Latent physical state	Mediator of effects
Y_k	Surface measurements	Diagnostic outputs
A_k	Influx disturbance	Target causal effect
B_k	Sensor bias states	Nuisance / confounder
C_k	Closure parameters	Mechanism modifier
H_k, T_k	Hydraulic and thermodynamic substates	Structured partition of X_k

Table 1 Core structural causal model variables and their roles.

der managed pressure drilling is fundamentally an interventional causal identification problem. The system is not observed under a single stationary regime but under a family of intervention regimes induced by routine choke and pump actions. If one can build a causal model that distinguishes which mechanisms should remain invariant across interventions and which are directly altered by do-operations, then one can exploit intervention diversity to separate influx-driven effects from actuation-driven effects. This is qualitatively different from conventional model-based filtering that treats inputs as known exogenous drivers and tries to fit residuals. In a causal identification approach, the objective is to isolate the causal effect of a latent influx disturbance on safety-relevant outputs, while adjusting for confounders that are themselves influenced by interventions and while respecting thermodynamic consistency of latent partitioning.

The technical contribution is an end-to-end causal-inference architecture with three coupled components [6]. The first component is a structural causal model (SCM) that formalizes annular hydraulics as a set of causal mechanisms linking interventions, latent inventories, and measurements. The SCM explicitly represents a dissolved inventory and swelling-mediated constitutive pathways, and it encodes which mechanisms are intervention-invariant. The second component is an invariant-causal learning objective that estimates these mechanisms from operational data by enforcing invariance of selected conditional distributions across intervention regimes and by penalizing predictive paths that change under do-operations. The third component is a counterfactual risk simulator that uses the learned SCM to compute distributions of bottomhole pressure deviation and surface-handling proxies under hypothetical interventions, enabling short-horizon decision support that is grounded in causal effect estimates rather than in raw correlations.

The remainder of the paper is organized into four main technical sections after this introduction. The next section formalizes the SCM and identifies the intervention structure induced by managed pressure drilling, clarifying how dissolution and swelling appear as latent variables and how closure uncertainty is represented within causal mechanisms. The following section derives an invariant-causal learning framework for estimating the SCM from mixed observational and interventional

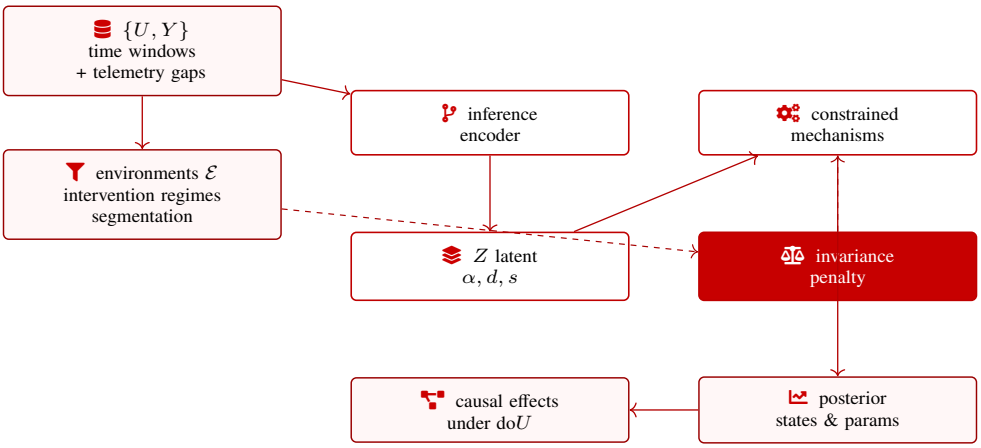


Figure 4 Invariant-causal learning stack. Operational data are partitioned into intervention-defined environments. A variational inference encoder estimates thermodynamics-augmented latent coordinates, while constrained mechanism layers learn stable mappings. An invariance penalty suppresses environment-specific predictive shortcuts, yielding posteriors suitable for causal effect estimation under explicit do-interventions.

State variable	Proxy contents	Dominant effect	Observability
p_k	Pressure node vector	Hydrostatic and storage response	Latent (inferred)
q_k	Mixture flow proxy	Frictional pressure loss	Partially observed
α_k	Free-gas holdup proxy	Compressible storage and density shift	Weakly observed
d_k	Dissolved-gas inventory	Swelling potential and solubility state	Latent
s_k	Swelling factor	Pit and density modification	Latent
T_k	Temperature proxy	Solubility trend and PVT context	Optional / sparse

Table 2 Latent hydraulic and thermodynamic state proxies in the dynamic SCM.

data, including constraints that enforce physically admissible phase partition and swelling behavior [7]. The next section develops counterfactual inference and risk estimation methods, showing how the causal model supports do-interventions for choke trajectories and how uncertainty is propagated to risk measures. The subsequent section addresses algorithms and numerical considerations, including identifiability, degeneracy under limited excitation, and computational strategies for stable online updates. A final section reports numerical studies and discussion, and the paper concludes with implications and limitations.

2. Structural Causal Model for Actuated Annular Hydraulics with Latent Partitioning

A structural causal model represents a system as a directed acyclic graph over variables with associated structural equations. In a time-evolving physical system, the natural representation is a dynamic SCM, in which variables at time t_k are linked to variables at time t_{k1} via causal mechanisms. For managed pressure drilling, the key distinction is between variables that are directly manipulated by the operator, variables that respond to those manipulations, and latent variables that influence measurements but are not directly observed. The causal identification problem is to infer the influence of a latent influx on outputs while accounting for the fact that interventions also influence many of the same outputs [8].

Let U_k denote the intervention vector at time t_k, including choke command, pump rate command, and any other boundary actuation signals. Let X_k denote the latent physical state, which is not fully observed but which includes pressure distribution proxies, mixture flow proxies, free-gas inventory proxies, dissolved-gas inventory proxies, and temperature proxies if needed. Let Y_k denote the measurement vector composed of surface pressure, standpipe pressure, flow-in, flow-out, and pit-volume change. Let B_k denote sensor bias states, such as pit calibration drift and flow meter scaling drift, and let C_k denote closure parameters, including friction multipliers and PVT scaling parameters. Let A_k denote an influx disturbance variable, representing gas mass entry rate and onset behavior. The SCM is defined by structural equations

$$\begin{aligned} X_{k1} &= fX_k, U_k, A_k, C_k\ \epsilon_k^x \\ Y_k &= hX_k, U_k, B_k\ \epsilon_k^y \\ B_{k1} &= gB_k\ \epsilon_k^b \\ C_{k1} &= C_k\ \epsilon_k^c \end{aligned} \tag{2.1}$$

where ϵ terms represent bounded or stochastic disturbances [9].

Mechanism	Schematic form	Intervention invariance	Notes
State dynamics	$X_{k1} = fX_k, U_k, A_k, C_k$	Partially invariant	Physics-driven, actuated by U_k
Measurement map	$Y_k = hX_k, U_k, B_k$	Locally invariant	Includes bias and actuator imprint
Dissolution relaxation	$d_{k1} = d_k \ \Delta t\, \kappa_d d^\star - d_k$	Invariant	Encodes solubility-driven partition
Swelling map	$s_k = Sd_k, p_k, T_k$	Invariant	Bounded monotone response
Bias drift	$B_{k1} = gB_k$	Slow drift	Models calibration and scaling errors
Closure drift	$C_{k1} = C_k \ \epsilon_k^c$	Very slow drift	Represents correlation mismatch

Table 3 Main structural mechanisms represented in the annular hydraulics SCM.

Environment e	MPD pattern	Intervention features	Identification purpose
e^{bp}	Quasi-steady backpressure	Small choke steps	Calibrate steady hydraulic response
e^{ramp}	Pressure ramps	Large, smooth choke moves	Excite compressible storage
e^{pump}	Pump transients	Pump start / stop / ramps	Separate pump and choke effects
e^{ch}	Choke oscillation tests	Designed backpressure cycles	Stress-test invariance assumptions
e^{conn}	Connections / off-bottom	Reduced flow, altered returns	Probe partition and swelling behavior

Table 4 Representative intervention-induced environments used for invariant learning.

The key causal distinction is that U_k is subject to interventions, so under a do-operation, the causal parents of U_k are removed and U_k is set externally. By contrast, A_k is not controlled and is treated as a disturbance with a prior distribution that may depend on geological context but not on U_k under the do-notation of managed pressure operations.

The SCM must represent dissolution and swelling as explicit mechanisms. To do so while remaining computationally tractable, the latent state X_k is partitioned into hydraulic variables H_k and thermodynamic partition variables T_k. The hydraulic variables include pressure node vector p_k, a flow proxy q_k, and a near-surface gas proxy α_k. The thermodynamic variables include a dissolved inventory proxy d_k and a swelling factor proxy s_k that modifies the mapping between mass and volume. The key structural relations are that (i) the dissolved inventory tends toward an equilibrium set by pressure and temperature, (ii) the swelling factor is a bounded monotone function of dissolved inventory, and (iii) the dissolved inventory and swelling factor influence measured pit-volume change and hydrostatics indirectly [10]. In reduced form, this can be expressed as

$$\begin{aligned} d_{k1} &= d_k \ \Delta t\, \kappa_d \left(d^\star p_k, T_k - d_k\right) \ \epsilon_k^d \\ s_k &= Sd_k, p_k, T_k; \theta_s \ \epsilon_k^s \end{aligned} \tag{2.2}$$

where $d^\star$ is an equilibrium map and S is a swelling map. Both maps are uncertain but bounded. The modeling objective in the SCM is not to specify these maps in high fidelity; it is to encode their directionality and boundedness so that the causal model does not attribute arbitrary pit trends to arbitrary latent states.

The SCM also encodes how free gas and dissolved gas partition affects hydraulic response. Free gas increases compressible storage and changes mixture density, influencing pressure transients under actuation. Dissolved gas affects density through swelling but has a different compressibility footprint [11]. This distinction is essential for separating swelling-driven pit gain from free-gas-driven compressibility under interventions. In the SCM, the hydraulic dynamics function f includes terms that map α_k and s_k into effective compressible storage and density. A typical reduced representation is a network model where pressure node updates depend on storage coefficients that vary with α_k and on hydrostatic coefficients that vary with s_k. This yields causal paths

$$U_k \to p_{k1}, \quad \alpha_k \to p_{k1}, \quad s_k \to p_{k1}, \quad A_k \to \alpha_{k1}, d_{k1}$$

while also allowing U_k to influence d_{k1} indirectly through p_k via the equilibrium map, reflecting that pressure interventions can shift dissolution.

Closure uncertainty enters through C_k, which influences friction and PVT relations. In a causal view, closure parameters modulate the strength of causal mechanisms rather than acting as additive noise [12]. For example, a friction multiplier changes the mapping from flow to pressure drop, and a gas density scaling changes the mapping from pressure to hydrostatic contribution. In the SCM, this is encoded by allowing f and h to depend on C_k, while also placing a prior on C_k and allowing it to drift slowly. The key reason for explicit C_k is to prevent the model from attributing all mismatch to influx or dissolution. If closure uncertainty is ignored, an estimator may attribute friction-induced pressure deviations to gas holdup changes, creating spurious causal effect estimates.

The measurement model h links latent states to observations. For pit-volume change, a relevant causal pathway is that swelling

Term	Sketch expression	Role in learning
Data fit	$-\log p_\theta y_k \mid z_k, u_k$	Match surface measurements
Invariance penalty	$\lambda_{\text{inv}} \|\mathbb{E}_e r_k - \mathbb{E} r_k\|^2$	Enforce stable mechanisms across e
Physics constraints	$\lambda_{\text{phy}} \Omega_{\text{phy}} z_k; \theta$	Bound partition and swelling behavior
Complexity / priors	KL or ℓ_1 penalties	Control model capacity and sparsity

Table 5 Components of the invariant-causal learning objective.

Mapping	Inputs	Structural property	Implementation sketch
Equilibrium $d^\star$	p, T	Bounded solubility surface	Shallow neural map with priors
Swelling S	d, p, T	Monotone in d, bounded	Monotone spline or positive weights
Fraction transform	Latent logits	Values in $0, 1$	Sigmoid mapping of unconstrained vars
Swelling factor	Latent scale	$s_k \geq 1$	$s_k = 1$ softplus$\cdot$
Closure scalings	Nominal PVT, friction	Limited range multipliers	Log-normal priors around unity

Table 6 Physically constrained latent mappings for partition and closure effects.

modifies volumetric return at surface for a given mass return, so pit change depends on flow imbalance and on swelling-induced density change. For pressure measurements, the dependence is more direct [13]. For flow-out measurements, the dependence includes both actual flow and sensor bias. The bias states B_k are included explicitly because biases can act as confounders: if pit bias drifts, the observation Y_k can shift in a way that correlates with interventions, producing spurious associations between actuation and inferred swelling. Modeling bias as a latent state introduces a causal pathway $B_k \to Y_k$ that can be adjusted for in causal effect estimation.

The SCM also clarifies which quantities can be treated as interventions and which as endogenous variables. Pump and choke commands are direct interventions. Measured casing pressure, however, is endogenous: it responds to choke behavior and to flow. This matters because naive adjustment can condition on endogenous variables that are colliders, thereby biasing causal effect estimates [14]. The SCM provides a principled way to identify adjustment sets for estimating the causal effect of influx A_k on outputs, and to avoid conditioning on variables that would open spurious paths.

To compute causal effects, the model must define do-operations on U_k. Under do$U_k = u$, the SCM replaces the structural equation for U_k with a constant assignment and removes incoming edges. Then the distribution of outputs under do can be computed by propagating the remaining structural equations. A schematic expression for the counterfactual distribution of an output functional R is

$$pR \mid dou_{0:K} = pR \mid X_{0:K}, u_{0:K}\, pX_{0:K} \mid dou_{0:K}\, dX_{0:K} \tag{2.3}$$

where $u_{0:K}$ denotes a planned intervention trajectory. This expression is the foundation for risk estimation later.

The challenge is identifiability: not all SCM parameters can be learned from surface data, and not all causal effects are identifiable without assumptions [15]. The present work adopts a strategy aligned with invariant causal prediction: learn only the mechanisms that can be validated as invariant across intervention regimes, and treat the rest as bounded nuisance mechanisms. This reduces overfitting and improves transportability across operating conditions. The next section develops this learning strategy and shows how invariance constraints are implemented while respecting physical bounds on partition and swelling.

3. Invariant-Causal Learning with Physically Constrained Mechanisms

Invariant causal prediction exploits the idea that causal mechanisms remain stable across environments, while spurious correlations can change when the environment changes. In managed pressure drilling, routine interventions naturally generate multiple environments: different choke settings, pump schedules, and backpressure profiles. These interventions change the distribution of some variables without changing the underlying causal mechanisms that map causes to effects, provided that the mechanism itself is not directly intervened upon [16]. The key idea is to find a representation and parameterization of the SCM such that the conditional distribution of specific variables given their causal parents is invariant across intervention regimes. This invariance can then be used both to learn mechanisms and to identify which predictive paths are causal rather than correlational.

Define environments $e \in \mathcal{E}$ as segments of operation characterized by intervention patterns, such as quasi-stationary backpressure segments, pump ramps, and choke transients. For each environment, data consists of sequences of U_k, Y_k and possibly intermittent downhole telemetry. The goal is to learn

Quantity	Definition sketch	Interpretation	Example use
$pR \mid dou$	Counterfactual output law	Distribution under planned trajectory	Compare alternative choke schedules
$\mathrm{VaR}_\alpha C$	Quantile of constraint C	α-level limit of excursion	Bound bottomhole deviation
$\mathrm{CVaR}_\alpha C$	Tail mean beyond VaR	Expected severity of rare events	Quantify worst-case MPD risk
$\Delta p_{\mathrm{bh}}^{\max}$	Max BHP deviation	Constraint on pressure envelope	Check kick tolerance
$\Delta V_{\mathrm{pit}}^{\max}$	Max pit excursion	Volumetric capacity margin	Assess trip tank / pit usage
$\gamma_{\mathrm{surf}}^{\max}$	Max surface gas proxy	Surface-handling intensity	Screen separator loading

Table 7 Counterfactual and risk quantities derived from the learned SCM.

Block	Input	Output	Key feature
Abduction encoder	Windowed U_k, Y_k	Posterior over latent Z_k	Intervention-conditioned inference
Latent dynamics smoother	Encoder outputs	Smoothed state trajectories	Uses dynamic SCM structure
Mechanism learner	Smoothed states, data	Updated θ	Invariance- and physics-regularized
Counterfactual simulator	θ, Z_k, proposed u	Samples of R	Abduction–action–prediction loop
Diagnostics module	Residuals, posteriors	Invariance and uncertainty flags	Detects misspecification and gaps

Table 8 Algorithmic blocks for online causal identification and prediction.

parameters θ of the SCM mechanisms such that, for selected target variables, the conditional likelihood is consistent across environments:

$$p_e Y_k \mid \mathrm{Pa} Y_k; \theta \approx p_{e'} Y_k \mid \mathrm{Pa} Y_k; \theta \tag{3.1}$$

for e, e' in a set of environments where the mechanism should be invariant. Here $\mathrm{Pa} Y_k$ denotes the causal parents of Y_k in the SCM. Enforcing invariance reduces the risk that the model uses environment-specific correlations to explain the data.

In practice, one does not know $\mathrm{Pa} Y_k$ exactly, and the SCM includes latent variables. The framework therefore focuses on learning an invariant latent representation Z_k that summarizes the aspects of X_k that causally influence Y_k and that are stable across environments [17]. The representation is thermodynamics-augmented: it includes explicit coordinates for free-gas proxy and dissolved inventory proxy, along with a swelling proxy that is constrained to be a bounded function of dissolved inventory and state. This explicit design choice reflects that a fully unconstrained latent representation can entangle swelling and free gas and can yield spurious invariances that do not correspond to physical mechanisms.

The learning objective combines three terms: a likelihood term that fits measurements, an invariance penalty that discourages environment-dependent residual structure, and a physical constraint penalty that enforces bounds and monotonicity of thermodynamic mechanisms. For a windowed dataset, a representative objective is

$$\begin{aligned} \mathcal{L}\theta = & \sum_{e \in \mathcal{E}} \sum_{k \in e} -\log p_\theta y_k \mid z_k, u_k \\ & \lambda_{\mathrm{inv}} \sum_{e \in \mathcal{E}} \| \mathbb{E}_e r_k \theta - \mathbb{E} r_k \theta \|^2 \\ & \lambda_{\mathrm{phy}} \sum_k \Omega_{\mathrm{phy}} z_k; \theta \end{aligned} \tag{3.2}$$

where $r_k \theta$ denotes standardized residuals, and Ω_{phy} penalizes violations of physical constraints such as bounds on partition variables and monotonicity of swelling with dissolved inventory. The invariance term encourages residual statistics to match across environments, reflecting that the mechanism should not change with the intervention regime once the correct causal parents are included.

A central issue is how to represent the thermodynamic partition without embedding an expensive equation-of-state solve. The approach adopted here uses a bounded equilibrium map $d^\star p, T; \theta^\star$ and a bounded swelling map $Sd, p, T; \theta_s$ with parametric forms constrained by priors [18]. The representation is selected so that it is expressive enough to capture uncertainty but constrained enough to avoid unphysical behavior. At this stage, the role of thermodynamic modeling literature is to motivate the inclusion of such maps and to inform plausible parameterization. Manikonda et al. (2021) [19] proposed an early thermodynamics-driven swelling model for drilling mud under kick scenarios, quantifying how dissolved gas can produce measurable volumetric expansion; this motivates treating swelling as a mechanistically structured response driven by a latent dissolved inventory, rather than as a free latent factor that could spuriously fit any pit trend.

To maintain bounds without hard clipping, partition vari-

Scenario	Description	Main confounder	Evaluation focus
Nominal MPD	Actuated, no influx	Friction and bias drift	False positives, baseline stability
Dissolution-buffered influx	Strong solubility, swelling	Similar early pit trends	Regime discrimination under buffering
Free-gas influx	Weak solubility, free gas	Compressible storage	Separation of gas vs actuation effects
Friction variability	Changing cuttings load	Pressure-only deviations	Robustness to friction mismatch
Pit bias drift	Slowly drifting pit offset	Apparent swelling	Need for explicit bias states
Closure mismatch	PVT / correlation errors	Structured model error	Uncertainty inflation and coverage

Table 9 Numerical scenario classes used in the simulation studies.

Limitation	Cause	Mitigation direction
Low intervention diversity	Narrow MPD operating band	Design gentle informational transients
Sparse sensing	Limited or delayed telemetry	Fuse extra channels when available
Closure uncertainty	Imperfect PVT and friction laws	Conservative priors and online scaling
Thermal gradients	Strong T variation with depth	Enrich temperature coupling in SCM
Operational adoption	Complexity of causal outputs	Simplified risk summaries and HMI design

Table 10 Key limitations of the present framework and suggested extensions.

ables are represented in transformed coordinates. For example, dissolved fraction and free-gas proxy are represented through sigmoid transforms of unconstrained variables, ensuring values lie in $0, 1$. Swelling factor is represented as 1 softplus$\cdot$ so it remains at least 1 while remaining differentiable. These transforms are embedded in the mechanism parameterizations, making the learning problem unconstrained in optimization variables while enforcing physical admissibility in the implied state.

Invariant learning must also respect intervention semantics [20]. Some mechanisms are directly affected by interventions. For example, the mapping from choke command to top pressure is not invariant across choke calibration regimes, and may drift. Such mechanisms should not be forced invariant across environments where the actuator behavior changes. The framework therefore constructs environment sets with respect to which invariance is enforced selectively. Mechanisms that represent physical transport and partition are enforced invariant across a broad set of environments, while actuator-related mechanisms are enforced invariant only within narrower operating bands or are treated as nuisance with larger uncertainty.

The causal identification objective also includes a constraint that discourages conditioning on colliders [21]. In a dynamic SCM, conditioning on measured outputs that are affected by both interventions and latent disturbances can open spurious backdoor paths. To mitigate this, the learning uses a restricted parent set: measurement likelihoods depend on current latent state and current intervention but not on future measurements, and the latent dynamics depend on interventions and latent disturbances but not directly on measurement residuals. This is consistent with a causal generative model and prevents certain forms of information leakage that can make the model appear invariant while actually exploiting acausal correlations.

Identifiability remains limited. Some parameter directions can be weakly identifiable without sufficient intervention diversity. The framework therefore introduces a controlled complexity principle: prefer simpler mechanisms unless the data across environments provides evidence that additional complexity is needed. This is implemented by sparsity-inducing penalties on mechanism parameters and by Bayesian priors that shrink parameters toward nominal [22]. When intervention diversity is sufficient, the invariance penalty encourages mechanisms that generalize across environments, and when diversity is insufficient, the priors prevent overinterpretation.

The output of invariant-causal learning is a learned SCM with a posterior over latent trajectories and over uncertain parameters, conditioned on observed data. This posterior supports counterfactual reasoning: one can compute how outputs would evolve under alternative interventions while holding latent disturbance realizations fixed. This is the core advantage of a causal formulation over a purely predictive formulation. The next section develops counterfactual inference and shows how it yields risk-relevant quantities for decision support, particularly in the presence of dissolution buffering and swelling ambiguity.

4. Counterfactual Inference and Short-Horizon Risk under Hypothetical Interventions

In managed pressure drilling, decisions often involve selecting among intervention options: hold backpressure, increase backpressure, reduce pump rate, or adjust choke trajectory to manage risk. A causal model enables counterfactual reasoning about

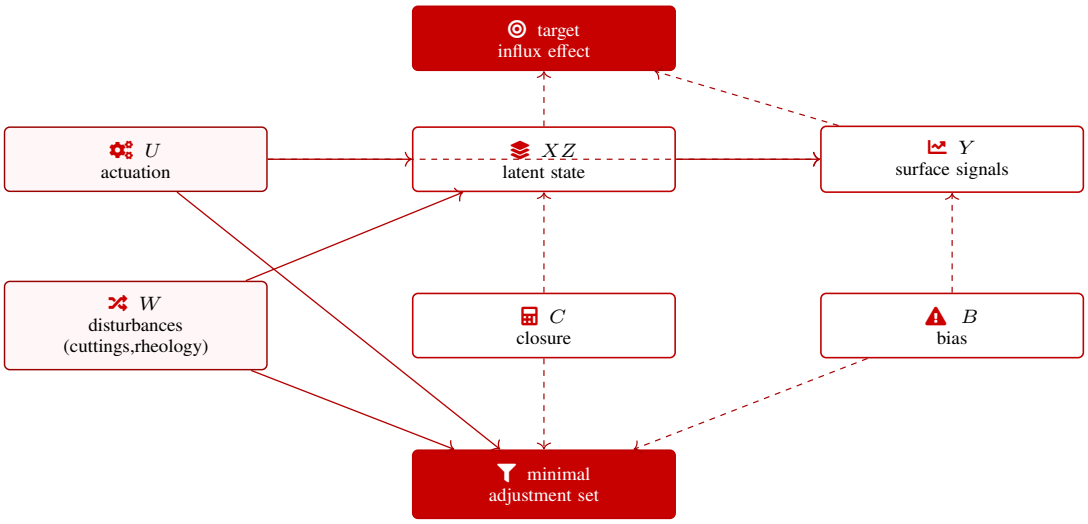


Figure 5 Constrained adjustment selection under partial observability. A compact causal skeleton highlights how interventions, disturbances, closure, and bias can all influence measurements. A constrained discovery layer selects a small adjustment set to estimate influx-relevant effects without conditioning on measurement pathways that would induce spurious associations under active control.

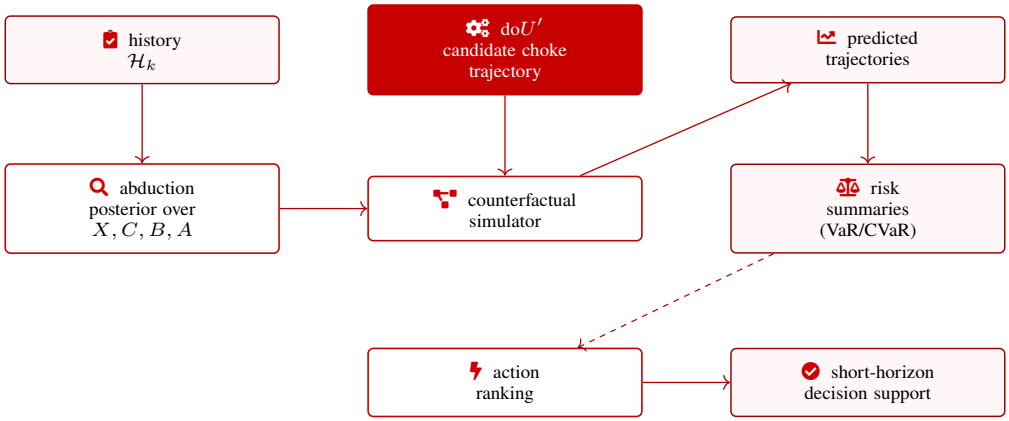


Figure 6 Counterfactual risk evaluation loop. Posterior abduction over latent inventories and uncertainties is followed by do-intervention simulation for candidate choke trajectories. Predicted trajectories feed risk summaries that support short-horizon action ranking, with dissolution-vs-free partition uncertainty propagated into tail-sensitive metrics.

these options: given the observed history and inferred latent states, what would the safety-relevant outputs have been under a different intervention trajectory? Counterfactual inference is particularly valuable in dissolution-buffered regimes, where the same observed pit gain can correspond to different latent partitions and where the effect of a pressure change depends on whether gas is free or dissolved [23].

The SCM supports counterfactuals through the abduction-action-prediction procedure. Abduction infers a posterior over latent variables and disturbances given observed data under the factual interventions. Action replaces the intervention structural equation with a new planned trajectory. Prediction propagates the system forward under the new intervention while sampling from the abducted posterior. The result is a distribution over counterfactual outcomes that reflects both state uncertainty and mechanism uncertainty.

Let $\mathcal{H}_k$ denote the observed history up to time t_k, including interventions and measurements. Let $u^f_{0:k}$ denote the factual intervention sequence and $u^{cf}_{k:kH}$ denote a proposed counterfactual intervention over a horizon H. Abduction yields a posterior $p\omega \mid \mathcal{H}_k$ over latent disturbances and initial state, where ω summarizes $A_{0:k}$, closure parameters, and latent initial conditions. The counterfactual outcome distribution for an output functional R is

$$pR \mid \mathcal{H}_k, dou^{cf} = pR \mid \omega, dou^{cf}\, p\omega \mid \mathcal{H}_k\, d\omega \tag{4.1}$$

where R may be a maximum bottomhole pressure excursion, a maximum surface gas proxy, or a pit-capacity excursion over the horizon [24].

A central technical issue is that counterfactual prediction must respect thermodynamic partition consistency. A pressure increase under a counterfactual choke trajectory can increase solubility and shift mass from free gas to dissolved inventory, which can reduce surface gas proxy risk while potentially increasing swelling and pit excursion risk. A pressure decrease can drive exsolution, potentially increasing free gas and surface risk.

These directional effects can be represented in the SCM through the equilibrium and relaxation mechanisms, but uncertainty in those mechanisms must be propagated. The counterfactual distribution therefore often exhibits multi-modal structure when partition uncertainty is large: one mode corresponds to buffering-dominant outcomes and another corresponds to free-gas-dominant outcomes. Rather than collapse this distribution to a mean, the framework computes risk measures that depend on tail behavior [25].

Risk measures are defined on functionals of the predicted output trajectories. For bottomhole pressure, a typical functional is the maximum deviation beyond bounds over the horizon. For surface handling, a functional is the maximum free-gas proxy at surface or the maximum gas volumetric outflow proxy. For pit volume, a functional is maximum pit excursion. For a generic constraint functional C, one can compute exceedance probability and conditional tail expectation:

$$\begin{aligned} \mathrm{VaR}_\alpha C &= \inf\{c : \mathbb{P}C \le c \ge \alpha\} \\ \mathrm{CVaR}_\alpha C &= \mathbb{E}C \mid C \ge \mathrm{VaR}_\alpha C \end{aligned} \tag{4.2}$$

These quantities can be computed from counterfactual samples. In a causal framework, these risk measures are conditioned on the observed history, so they represent a posterior predictive risk given current information [26].

Counterfactual evaluation can be used not only to compute risk but also to compute causal effect measures: how much does a proposed intervention reduce expected surface gas proxy or increase expected pit excursion? Such effect measures can guide decision support in a multi-objective setting where constraints trade off. The framework emphasizes that these effects are not purely correlational; they are computed under do-operations on interventions, holding latent disturbances fixed. This allows one to attribute changes to interventions rather than to co-occurring disturbances.

Computationally, counterfactual prediction requires repeatedly simulating the SCM under different interventions. Because the SCM is a reduced model with learned mechanisms, simulation is cheap enough for short horizons. However, uncertainty propagation can be costly if naive Monte Carlo is used. The framework therefore uses structured sampling: it samples a limited set of disturbance scenarios that cover posterior uncertainty directions most relevant to risk, as determined by the posterior covariance and sensitivity of constraint functionals [27]. This is a targeted ensemble approach. Additionally, for small perturbations in intervention trajectories, local linearization of the SCM around the current posterior mode can yield fast approximations of expected effects, while full nonlinear samples are reserved for evaluating tail risk.

A practical concern is that counterfactual predictions can be fragile if the learned mechanisms are not valid under the proposed interventions. The invariant-causal learning stage mitigates this by preferring mechanisms that are stable across observed intervention regimes. Yet counterfactual interventions may explore slightly different regimes. The framework therefore restricts counterfactuals to admissible intervention classes defined by operational constraints and observed regime coverage. When counterfactuals extend beyond coverage, the model inflates uncertainty and reports lower confidence rather than producing sharp predictions [28].

Counterfactual inference is also useful for distinguishing swelling-driven pit gain from free-gas-driven pit gain. Consider a factual history in which pit gain increases under nominal backpressure. The SCM posterior may assign probability mass to both high-dissolved and high-free regimes. A counterfactual increase in pressure can have opposite effects in these regimes: in a swelling-buffered regime, increased pressure can increase solubility and increase swelling contribution, potentially increasing pit gain while reducing free gas; in a free-gas regime, increased pressure compresses free gas and can reduce pit gain and surface gas proxy. By simulating both regimes under the counterfactual and comparing predicted measurement signatures, one can design an informational intervention. The present paper does not propose an explicit control policy, but it shows that the causal model naturally supports such informational counterfactuals, and it can quantify how an intervention would reduce regime ambiguity [29].

The next section addresses the algorithmic implementation of learning and counterfactual inference, including sparse optimization, online updates, and numerical stability under inequality constraints and partial observability. It also discusses identifiability limits and failure modes, which are central for responsible decision support.

5. Algorithms, Identifiability, and Numerical Stability for Online Deployment

Implementing a causal identification layer in drilling requires attention to computational constraints and to identifiability under partial observability. A model that is theoretically appealing but numerically unstable under real sensor conditions is not useful. This section presents algorithmic strategies that maintain stability and provides a structured discussion of identifiability limits inherent in the problem.

The learning problem combines latent state inference with mechanism parameter learning under invariance constraints. This is naturally posed as a constrained variational inference problem, where the posterior over latent trajectories and parameters is approximated [30]. The objective combines a data likelihood with priors and invariance penalties. A practical algorithm is intervention-conditioned amortized variational inference: an encoder maps windows of measurements and interventions to posterior parameters for latent variables, while mechanism parameters are learned by maximizing an evidence lower bound augmented with invariance penalties. Amortization yields fast online inference, while maintaining a mechanism model that is shared across time.

However, unconstrained amortization can violate physical bounds. To prevent this, the latent variables corresponding to partition and swelling are parameterized with bound-preserving transforms, and the encoder outputs unconstrained parameters that map into admissible ranges. The mechanism models similarly use parameterizations that guarantee monotonicity where needed. For example, the swelling map is parameterized so its derivative with respect to dissolved inventory is nonnegative

over the range [31]. This can be achieved by expressing the derivative as a positive function and integrating, or by using monotone spline parameterizations with positive coefficients. These design choices reduce the risk that the learned model uses physically implausible paths to satisfy invariance penalties.

Optimization is performed with alternating updates: latent trajectories are updated given current mechanisms, then mechanisms are updated given latent trajectories, with invariance penalties computed over environments. Because environments are defined by intervention regimes, minibatching by environment ensures that invariance gradients are informative. To avoid degenerate solutions where the model forces invariance by making outputs insensitive to inputs, the objective includes a predictive adequacy term and a mechanism complexity penalty that discourages trivial solutions. Additionally, counterfactual validity checks are used: mechanisms are tested on held-out intervention regimes to ensure they generalize.

Identifiability is limited by the nature of available sensors [32]. Without downhole measurements, pressure distribution proxies are weakly identifiable, and free vs dissolved partition can be ambiguous because both affect pit volume and pressure in coupled ways. The causal framework does not eliminate this ambiguity; it quantifies it. The posterior may remain broad in certain directions. The operational value lies in recognizing when ambiguity is intrinsic and avoiding overconfident decisions. The framework provides diagnostics based on posterior covariance and on invariance residuals. If invariance residuals remain high across environments, this suggests the mechanism model is misspecified or that the assumed parent set is incorrect [33]. If posterior covariance remains large despite diverse interventions, this suggests an information limitation.

A key confounder is friction variability. Friction changes can mimic certain pressure deviations that would otherwise indicate gas holdup. If friction is modeled as a latent drift parameter, it can absorb deviations and reduce spurious influx inference, but it can also reduce sensitivity to real influx if friction is allowed to vary too freely. The causal approach addresses this by using invariance: friction mechanisms should be stable across environments in their functional form, even if their parameter drifts slowly. By penalizing environment-specific friction behavior, the model is encouraged to attribute deviations that correlate with interventions to actuation paths, and deviations that persist across intervention changes to latent disturbances. This does not guarantee correct attribution, but it improves robustness [34].

Numerical stability is enhanced by using smoothing rather than filtering. Filtering updates can be brittle when measurements are correlated and when model mismatch is present. Smoothing over a sliding window allows the model to use future observations to disambiguate current latent states, which is especially valuable under intermittent telemetry. The causal learning and inference can be implemented as a windowed smoother, with states and disturbances over the window jointly inferred. Sparsity arises because dynamics factors connect consecutive time steps, enabling efficient Gauss–Newton updates. The variational representation can exploit this sparsity by using a banded precision structure.

Intervention semantics also help numerical stability [35]. By explicitly representing U_k as intervened variables, the model avoids learning spurious feedback from measurements to interventions, which would be acausal and destabilizing in online deployment. The model uses the known intervention trajectory as an exogenous signal. When intervention commands differ from realized actuator behavior due to delays or nonlinearities, actuator states can be modeled explicitly as additional latent variables driven by commands, preserving causality while capturing actuator dynamics.

The algorithm must also handle missing data. Missing measurements are common in drilling due to sensor dropouts. In a probabilistic model, missing data corresponds to absent likelihood factors. The posterior then contracts less, but inference remains defined [36]. Uncertainty grows under missing data, which is appropriate. When data resumes, smoothing over the window re-incorporates it. This is more stable than ad hoc imputation, because the model explicitly propagates uncertainty rather than filling missing values with point estimates.

Finally, the system must be robust to property-model mismatch. Because PVT properties can be uncertain and correlation errors can persist, the model includes PVT scaling parameters with priors. These parameters modulate density and viscosity within plausible bounds [37]. The causal approach uses intervention variation to reduce sensitivity to these parameters by learning invariances that hold across regimes. When uncertainty remains, the posterior reflects it, and counterfactual risk estimates include it. This is preferable to a deterministic model that hides mismatch inside state estimates.

The next section reports numerical studies that evaluate the causal identification framework in scenarios designed to stress managed pressure actuation, dissolution buffering, friction variability, and sensor bias. The focus is on regime discrimination, counterfactual risk differences, and stability under limited telemetry.

6. Numerical Studies and Discussion

The numerical studies are designed to evaluate whether an interventional causal identification approach can provide practical benefits relative to purely correlational or purely residual-based approaches in managed pressure drilling settings. The studies use synthetic datasets generated from a separate simulator that includes compressible hydraulics, frictional pressure losses, and a partitioning mechanism between free and dissolved gas with swelling effects [38]. The causal model used for inference is intentionally reduced and includes uncertainty in closure parameters to reflect realistic mismatch.

Several classes of scenarios are considered. In nominal scenarios, there is no influx, but managed pressure actuation is active, including choke steps, ramps, and pump changes. Friction varies slowly due to cuttings loading. Sensor bias drifts slowly in pit measurement. The objective is to test false positives and baseline stability. In influx scenarios, an influx occurs with uncertain onset and magnitude [39]. Two regimes are emphasized: a dissolution-buffered regime with strong solubility and swelling effects, and a free-gas-dominated regime

with weak solubility. Actuation continues in both regimes, and the goal is to test whether the causal approach can separate actuation-induced transients from influx-induced effects, and whether it can distinguish buffered swelling-driven pit gain from free-gas-driven compressibility patterns.

In nominal scenarios, the model learns invariant mechanisms across intervention regimes and yields posterior distributions over latent variables that remain concentrated near nominal. The invariance penalty suppresses spurious predictive paths that would otherwise attribute certain actuation-induced pit variations to gas inventory changes, because those paths fail to remain invariant across different intervention patterns. The posterior over friction parameters adapts slowly, and the posterior over pit bias accounts for drift. The result is that the inferred influx disturbance remains near zero with high probability, and counterfactual risk estimates for near-term surface gas handling remain low. This baseline behavior is essential for operational use because frequent false alarms under routine actuation would render any decision support system unusable [40].

In dissolution-buffered influx scenarios, early pit gain arises primarily from swelling-driven volumetric return changes while free-gas holdup remains limited. Surface pressure responses can be modest and confounded with actuation. The causal model assigns posterior mass to increased dissolved inventory and increased swelling proxy while keeping free-gas proxy relatively bounded. This assignment is not based on pit gain alone; it arises because invariance across intervention regimes rejects explanations in which pit gain is produced by free-gas compressibility when pressure interventions should have produced a different signature under that regime. In counterfactual evaluation, a pressure-increasing choke trajectory produces predicted reductions in free-gas proxy while potentially increasing pit excursion risk, whereas a pressure-decreasing trajectory increases free-gas proxy risk. These counterfactual differences are consistent with the model's partition structure and provide a basis for regime-sensitive decision support [41].

In free-gas-dominated influx scenarios, the posterior shifts toward increased free-gas proxy and increased compressible storage proxy, with a smaller increase in dissolved inventory. Pressure and flow coupling features become more informative because free gas affects pressure transients more directly. In these scenarios, counterfactual pressure-increasing trajectories reduce predicted surface gas proxy and reduce pit gain, reflecting compression of free gas. The causal effect estimates differ from buffered scenarios, and the model's regime diagnostic based on partition posteriors reflects that difference. Importantly, the causal model does not need to perfectly simulate migration to provide this distinction; it relies on invariance across intervention regimes and on causal partition pathways that constrain how pit and pressure should co-vary.

Friction variability scenarios test confounding. When friction increases without influx, pressure rises and flow-out changes can resemble influx signatures [42]. A correlational detector can misclassify such scenarios. The causal model represents friction as a mechanism parameter that can drift slowly. Because friction affects pressure in a way that remains consistent across intervention regimes, the invariance constraint encourages the model to attribute pressure deviations that persist across interventions to friction rather than to influx. This reduces spurious influx posterior mass. When an influx is present concurrently with friction change, ambiguity increases, and the posterior reflects it rather than collapsing. This is a central objective: to avoid overconfident misattribution when the data does not support a unique explanation.

Sensor bias scenarios evaluate robustness [43]. Pit bias drift can mimic swelling-driven pit gain if not modeled. The causal framework includes explicit bias states and penalizes rapid bias changes through priors. When pit drift is slow and consistent with bias dynamics, the model attributes it to bias rather than to swelling. When pit changes correlate with pressure and flow patterns inconsistent with bias-only explanations, the model shifts posterior mass toward swelling or free gas as appropriate. This demonstrates that explicit bias modeling is not optional in this setting; it is required to prevent spurious causal conclusions.

Closure mismatch scenarios examine the influence of PVT scaling uncertainty. When gas density mapping is perturbed in the data generator, pressure predictions shift [44]. If the causal model ignores this, it may attribute pressure mismatch to gas inventory changes. By including PVT scaling parameters with priors, the causal model can attribute part of the mismatch to closure uncertainty, widening posterior intervals for risk measures. This yields more conservative counterfactual risk estimates, which is preferable to confident but wrong decisions. The trade-off is that uncertainty can remain large, highlighting the value of additional sensing or of more informative intervention diversity.

Ablation studies illustrate which components of the framework are essential. Removing invariance penalties increases sensitivity to environment-specific correlations and increases false positives under actuation [45]. Removing thermodynamic partition structure causes the model to conflate swelling and free gas, reducing interpretability and distorting counterfactual risk directionality under pressure changes. Removing explicit bias states causes pit drift to be misattributed to swelling, increasing false buffered-influx diagnoses. These ablations reinforce that the causal formulation is not a single trick; it is an integrated design in which intervention semantics, invariant learning, and physically constrained latent partition jointly reduce ambiguity.

The studies also highlight limitations. If intervention diversity is low, invariance provides limited leverage because environments are not sufficiently different to reveal spurious correlations. If the system operates nearly at steady conditions with minimal pressure modulation, dissolution-buffered and free-gas regimes can remain difficult to distinguish from surface data alone. In such cases, the model reports broad posteriors and counterfactual risk intervals that overlap, reflecting limited information [46]. This is an honest representation of uncertainty rather than a failure, but it implies that operational decisioning must rely on conservative policies or on targeted informational interventions. The causal model can quantify which interventions would be most informative by computing expected differences in counterfactual signatures between regimes, though implementing such interventions must respect safety constraints.

Overall, the numerical studies indicate that treating managed

pressure drilling diagnosis as an interventional causal identification problem can improve robustness to actuation-induced transients and can yield regime-sensitive counterfactual risk assessments that distinguish swelling-buffered behavior from free-gas-dominated behavior under identical early pit trends. The causal approach does not eliminate the need for physical modeling; it reuses physical structure in a way that supports invariance and counterfactual reasoning.

7. Conclusion

This paper developed an interventional causal identification framework for diagnosing dissolution-buffered gas influx in managed pressure drilling. The core contribution was a structural causal model that explicitly represents partitioned gas inventories, swelling-mediated constitutive pathways, actuator interventions, sensor biases, and closure uncertainties as distinct mechanisms, enabling causal effect estimation under do-operations on choke and pump trajectories. An invariant-causal learning objective was derived to exploit routine intervention diversity as quasi-experimental variation, enforcing stability of key mechanisms across operating environments while penalizing spurious predictive paths that fail under intervention shifts [47]. Thermodynamics-augmented latent variables were parameterized with bound-preserving transforms and physically constrained mechanisms to prevent unphysical explanations for pit and pressure patterns, enabling regime diagnostics that separate swelling-consistent pit gain from free-gas-driven compressibility patterns. Counterfactual inference was then used to compute short-horizon risk distributions under hypothetical interventions, supporting decision support based on causal effect estimates rather than on correlation-driven alarms.

The framework was motivated by structural ambiguity in early-stage signals and by the need for stability under persistent actuation and closure mismatch. Manikonda et al. (2020) [3] and Manikonda et al. (2021) [19] provided early thermodynamic modeling pathways for, respectively, quantifying kick-gas dissolution in oil-based drilling fluids and characterizing kick-induced mud swelling, and the present work leveraged those conceptual mechanisms as constrained latent structure rather than as central objects of study. Remaining limitations arise from intrinsic observability constraints under sparse sensing and limited intervention diversity, and from the need to calibrate uncertainty envelopes for closure parameters conservatively, especially when property correlations exhibit residual errors. Future work can integrate richer temperature coupling when thermal variation is a dominant driver of solubility over the relevant horizon, incorporate additional telemetry channels when available, and couple causal risk estimates to risk-aware actuation policies that explicitly balance safety and information gain. Within the present scope, interventional causality offers a principled route to make managed pressure drilling diagnosis more robust, interpretable, and aligned with the decision structure imposed by continuous boundary actuation [48].

Acknowledgments

We would like to thank the reviewers of this research for their helpful comments and suggestions.

References

[1] J. R. Bhatt and M. George, "Neutrino induced vorticity, alfven waves and the normal modes," *The European Physical Journal C*, vol. 77, pp. 539–, 8 2017.

[2] K. K. Fjelde, Øystein Arild, and T. Loberg, "An integrated approach to risk- and hydraulic simulations in a well control planning perspective," in *IADC/SPE Asia Pacific Drilling Technology Conference and Exhibition*, SPE, 11 2006.

[3] K. Manikonda, A. R. Hasan, O. Kaldirim, N. Rahmani, and M. A. Rahman, "Estimating swelling in oil-based mud due to gas kick dissolution," in *International conference on offshore mechanics and arctic engineering*, vol. 84430, p. V011T11A039, American Society of Mechanical Engineers, 2020.

[4] K. Bybee, "Managed-pressure drilling: Kick detection and well control," *Journal of Petroleum Technology*, vol. 62, pp. 57–58, 1 2010.

[5] A. K. Sleiti, W. A. Al-Ammari, M. Abdelrazeq, M. El-Naas, M. A. Rahman, A. Barooah, R. Hasan, and K. Manikonda, "Comprehensive assessment and evaluation of correlations for gas-oil ratio, oil formation volume factor, gas viscosity, and gas density utilized in gas kick detection," *Journal of Petroleum Science and Engineering*, vol. 207, p. 109135, 2021.

[6] W. S. McMillan, "Overcoming drilling challenges in northwest china using an innovative mpd technique," in *SPE/IADC Managed Pressure Drilling and Underbalanced Operations Conference and Exhibition*, SPE, 2 2010.

[7] L. Nokleberg, R. B. Schulle, and T. Sontvedt, "Shallow gas kicks, safety aspects related to diverter system," *SPE Offshore Europe*, 9 1987.

[8] A. Hale and A. K. R. Dewan, "Inhibition of gas hydrates in deepwater drilling," *SPE Drilling Engineering*, vol. 5, pp. 109–115, 6 1990.

[9] X. Tang, L. Dou, R. Wang, J. Wang, S. Wang, J. Wang, and J. Shi, "Innovations of gas lift in prolific, long-perforations, and multilayered wells, case study in sudan," in *SPE/AAPG Africa Energy and Technology Conference*, SPE, 12 2016.

[10] J. H. Bardarson and C. W. J. Beenakker, "Degradation of electron-hole entanglement by spin-orbit coupling," *Physical Review B*, vol. 74, pp. 235307–, 12 2006.

[11] I. Sule, F. Khan, and S. Butt, "Experimental investigation of gas kick effects on dynamic drilling parameters," *Journal of Petroleum Exploration and Production Technology*, vol. 9, pp. 605–616, 6 2018.

[12] B. W. Atchison, "Automated well control: From automated detection to automated shut-in," in *SPE/IADC Middle East Drilling Technology Conference and Exhibition*, SPE, 5 2021.

[13] Q. Zhou, H. Zhao, S. Li, Y. He, and H. Zhang, "An improved gas kick detection method based on continuous doppler ultrasonic wave in deep water drilling," *Advances in Mechanical Engineering*, vol. 9, pp. 168781401771542–, 8 2017.

[14] J. Marklof, "Kinetic limits of dynamical systems," 8 2014.

[15] B. Zhao, Z.-Y. Li, F. Nakamura, R. Krasnopolsky, and H. Shang, "Magnetic flux expulsion in star formation," *The Astrophysical Journal*, vol. 742, pp. 10–, 11 2011.

[16] J. R. Tangstad, "Assessment of dynamic barriers in oil/-gas well operations: Vurdering av dynamiske barrierer i olje/gass brønner," 1 2014.

[17] M. El-Sayed, A. Ezz, M. Aziz, and S. A. Waheed, "Successes in curing massive lost circulation problems with a new expansive lcm," in *SPE/IADC Middle East Drilling and Technology Conference*, SPE, 10 2007.

[18] P. Skalle and A. L. Podio, "Trends extracted from 800 gulf coast blowouts during 1960-1996," *IADC/SPE Drilling Conference*, 3 1998.

[19] K. Manikonda, A. R. Hasan, N. H. Rahmani, O. Kaldirim, C. E. Obi, J. J. Schubert, and M. A. Rahman, "A gas kick model that uses the thermodynamic approach to account for gas solubility in synthetic-based mud," in *SPE/IADC Middle East drilling Technology conference and exhibition*, p. D031S016R001, SPE, 2021.

[20] A. Judzis and A. Poddar, "R&d grand challenges - reviewing the five r&d grand challenges plus one," *Journal of Petroleum Technology*, vol. 64, pp. 69–73, 9 2012.

[21] K. K. Nassab, S. Z. Ting, S. Buapha, N. MatNoh, and M. N. Hemmati, "How to improve accuracy of a kick tolerance model by considering the effects of kick classification, frictional losses, pore pressure profile, and influx temperature," *SPE Drilling & Completion*, vol. 37, pp. 15–25, 11 2021.

[22] G. Karras, E. Hertz, F. Billard, B. Lavorel, J.-M. Hartmann, O. Faucher, E. Gershnabel, Y. Prior, and I. S. Averbukh, "Orientation and alignment echoes.," *Physical review letters*, vol. 114, pp. 153601–, 4 2015.

[23] R. J. Lunn, "Options for scotland's gas future," 6 2015.

[24] B. Zakeri, L. Barreto-Gomez, B. Boza-Kiss, L. G. Echeverri, S. Fritz, D. Gielen, R. Ghoneim, S. Pachauri, K. Paulavets, J. Rogelj, L. Srivastava, and C. Zimm, "Bouncing forward sustainably: Pathways to a post-covid world. sustainable energy," 6 2020.

[25] I. Sarsenov, A. Blackman, and S. A. M. Obeyesekere, "Papua new guinea economic update : Slower growth, better prospects," 1 2019.

[26] T. Lee, K. Lee, K. Sung, and J. Choe, "Well control modeling of oil based mud for various well trajectories," *Journal of the Korean Society of Mineral and Energy Resources Engineers*, vol. 50, pp. 482–489, 8 2013.

[27] C. Leach and P. Stanton, "Deep water development drilling from a spar," in *Offshore Technology Conference*, OTC, 5 1999.

[28] R. J. Ragan, W. J. Mullin, and E. B. Wiita, "Landau damping of spin waves in trapped boltzmann gases," *Journal of Low Temperature Physics*, vol. 138, pp. 693–698, 2 2005.

[29] D. Gomes, K. S. Bjorkevoll, K. K. Fjelde, and J. Frøyen, "Numerical modelling and sensitivity analysis of gas kick migration and unloading of riser," in *Volume 8: Polar and Arctic Sciences and Technology; Petroleum Technology*, American Society of Mechanical Engineers, 6 2019.

[30] O. Weustink, "Bombax 48-inch pipeline installation," in *Offshore Technology Conference*, OTC, 5 2003.

[31] A. F. Ibrahim, A. I. Assem, M. Ibrahim, and C. Pieprzica, "Water flowback rta analysis to estimate fracture geometry and rank the shale quality," in *SPE Latin American and Caribbean Petroleum Engineering Conference*, SPE, 7 2020.

[32] A. A. Ghauri, K. K. Fjelde, and J. Frøyen, "A transient model for hydraulic simulation of bullheading and pressurized mud cap drilling," in *Volume 8: Polar and Arctic Sciences and Technology; Petroleum Technology*, American Society of Mechanical Engineers, 6 2016.

[33] G. Z. Han, L. Lemesany, A. A. Azizov, and F. DeLeon, "Practical directional drilling techniques in pinedale field wyoming to improve drilling performance," in *SPE Unconventional Resources Conference Canada*, SPE, 11 2013.

[34] M. Williamson and R. Dawe, "Mud-gas separator response to well control procedure," *IADC/SPE Drilling Conference*, 2 1994.

[35] I. Mills, D. Reitsma, J. Hardt, and Z. Tarique, "Simulator and the first field test results of an automated early kick detection system that uses standpipe pressure and annular discharge pressure," in *SPE/IADC Managed Pressure Drilling and Underbalanced Operations Conference and Exhibition*, SPE, 3 2012.

[36] H. Müntinga, H. Ahlers, M. Krutzik, A. Wenzlawski, S. E. Arnold, D. Becker, K. Bongs, H. Dittus, H. Duncker, N. Gaaloul, C. Gherasim, E. Giese, C. Grzeschik, T. W. Hänsch, O. Hellmig, W. Herr, S. Herrmann, E. Kajari, S. Kleinert, C. Lämmerzahl, W. Lewoczko-Adamczyk, J. I. Malcolm, N. Meyer, R. J. M. Nolte, A. Peters, M. Popp, J. Reichel, A. Roura, J. Rudolph, M. Schiemangk, M. Schneider, S. T. Seidel, K. Sengstock, V. Tamma, T. Valenzuela, A. Vogel, R. Walser, T. Wendrich, P. Windpassinger, W. Zeller, T. van Zoest, W. Ertmer, W. P. Schleich, and E. M. Rasel, "Interferometry with bose-einstein condensates in microgravity," *Physical review letters*, vol. 110, pp. 093602–093602, 2 2013.

[37] A. Samuels, "H2s need not be deadly, dangerous, destructive," in *SPE Symposium on Sour Gas and Crude*, SPE, 11 1974.

[38] J. Maršálek, P. Brož, and M. Bobák, "Complex biogas membrane upgrading to biocng at agriculture biogas plant," *Chemical Papers*, vol. 74, pp. 4227–4239, 6 2020.

[39] P. Ramljak, "Razdjelnik podesive sapnice," 1 2019.

[40] J. Guedes, P. Madau, L. Mayer, and S. Callegari, "Recoiling massive black holes in gas-rich galaxy mergers," *The Astrophysical Journal*, vol. 729, pp. 125–, 2 2011.

[41] Y. Ding, Z. Huang, and L. Wang, "2d optical streaking for ultra-short electron beam diagnostics," 12 2011.

[42] Y.-J. Xu, "Selective oxidation of hydrocarbons using supported gold, silver, copper and bimetallic catalysts," 9 2006.

[43] T. Bogdanovic, C. S. Reynolds, and M. C. Miller, "Alignment of the spins of supermassive black holes prior to coalescence," *The Astrophysical Journal*, vol. 661, pp. 1–L150, 5 2007.

[44] S. Solem and S. Evje, "Relaxation limit of a compressible gas–liquid model with well–reservoir interaction," *Zeitschrift für angewandte Mathematik und Physik*, vol. 68, pp. 23–, 1 2017.

[45] L. Oyarte-Gálvez and D. van der Meer, "Granular motor in the non-brownian limit," *Journal of Statistical Mechanics: Theory and Experiment*, vol. 13, pp. 043206–, 4 2016.

[46] I. Jamaludin, A. A. Masngot, M. H. Basir, A. Abdullah, A. Z. A. Murad, and D. Arsanti, "Ior in a waxy, marginal fields, offshore malaysia environment; past efforts and future outlook – a case study," in *Offshore Technology Conference*, OTC, 5 2020.

[47] J. P. Donnelly, "Comments: In search of profitability," *Journal of Petroleum Technology*, vol. 71, pp. 12–12, 7 2019.

[48] R. M.J., A. A.R., L. T., and S. J.M., "Foundation integrity: Shallow gas mitigation using the xpp monitoring tool - an offshore malaysia case history," in *Offshore Technology Conference-Asia*, OTC, 3 2014.